

Microcanonical Transition State Theory for Activated Gas–Surface Reaction Dynamics: Application to H₂/Cu(111) with Rotation as a Spectator

Heather L. Abbott and Ian Harrison*

Department of Chemistry, University of Virginia, Charlottesville, Virginia 22904-4319

Received: May 24, 2007; In Final Form: July 13, 2007

A microcanonical unimolecular rate theory (MURT) model incorporating quantized surface vibrations and Rice–Ramsperger–Kassel–Marcus rate constants is applied to a benchmark system for gas–surface reaction dynamics, the activated dissociative chemisorption and associative desorption of hydrogen on Cu(111). Both molecular translation parallel to the surface and rotation are treated as spectator degrees of freedom. MURT analysis of diverse experiments indicates that one surface oscillator participates in the dissociative transition state and that the threshold energy for H₂ dissociation on Cu(111) is $E_0 = 62$ kJ/mol. The spectator approximation for rotation holds well at thermally accessible rotational energies (i.e., for E_r less than ~ 40 kJ/mol). Over the temperature range from 300 to 1000 K, the calculated thermal dissociative sticking coefficient is $S_T = S_0 \exp(-E_a/k_B T)$ where $S_0 = 1.57$ and $E_a = 62.9$ kJ/mol. The sigmoid shape of rovibrational eigenstate-resolved dissociative sticking coefficients as a function of normal translational energy is shown to derive from an averaging of the microcanonical sticking coefficient, with threshold energy E_0 , over the thermal surface oscillator distribution of the gas–surface collision complexes. Given that H₂/Cu(111) is one of the most dynamically biased of gas–surface reactive systems, the simple statistical MURT model simulates and broadly rationalizes the H₂/Cu(111) reactive behavior with remarkable fidelity.

I. Introduction

The allure of transition state theories (TSTs) of chemical reactivity is that they can often reduce complicated considerations of multidimensional reaction dynamics to a simpler accounting of the reactive flux that passes through the transition state along the minimum energy pathway separating reactants and products. Despite the overwhelming success of Rice–Ramsperger–Kassel–Marcus (RRKM) theory for the treatment of unimolecular reactions of polyatomic molecules in the gas phase,^{1,2} the utility of the microcanonical unimolecular rate theory (MURT; a TST) for treating the dynamics of activated gas–surface reactions has not been broadly recognized. Although instances of vibrational mode-specific reactivity in methane dissociative chemisorption on Ni surfaces have been observed,^{3,4} it remains under active investigation whether such mode-specific reactivity is exceptional, as would be the case for larger polyatomic molecules in the gas phase,^{1,5} or whether mode-specific gas–surface reactivity will significantly effect thermal rate constants that are averaged over many quantum states.^{6,7} Rapid progress in generalized gradient approximation density functional theory (GGA-DFT) makes it possible to calculate increasingly accurate reactive potential energy surfaces (PESs) for gas–surface reactions at a surface temperature of $T_s = 0$ K.⁸ Unfortunately, a versatile full dimensionality kinetics framework to connect nonequilibrium dynamical experiments to transition state or reactive PES characterization has been largely lacking.^{9,10} The MURT is one approach to provide this connection between $T_s \neq 0$ K experiments and PES characterization and is formulated in such a way as to naturally include surface phonons and as many molecular degrees of freedom as needed.

In this paper, a simple statistical MURT model with three parameters is shown to reproduce many aspects of the activated dissociative chemisorption and associative desorption of hydrogen on Cu(111), a benchmark system for gas–surface reaction dynamics for which the breadth of detailed and quantum-state-resolved experimental data is unsurpassed.^{11–14} The dynamics of the thermal associative desorption of hydrogen from Cu(111) have been particularly well-characterized by gas-phase measurements of desorbing hydrogen (e.g., angular yields and quantum-state-resolved energy distributions). The principle of detailed balance at thermal equilibrium allows the hydrogen dissociative chemisorption dynamics to be calculated given knowledge of the associative desorption dynamics¹¹ and vice versa. Although the H₂/Cu(111) reactive system is dynamically biased and does not behave completely statistically, the MURT model still provides a useful conceptual framework by which to understand and simulate the reaction dynamics. Experiments find that the dissociative sticking coefficient, S , of hydrogen on Cu(111) scales with the molecular translational energy directed along the surface normal. This normal translational energy is $E_n = E_t \cos^2 \vartheta$ for molecules with translational energy E_t incident upon the surface at an angle ϑ from the surface normal. The scaling of S with E_n implies that molecular translation parallel to the surface is a spectator to the hydrogen dissociation dynamics. Rotational motion is also approximately a spectator at thermally accessible energies (i.e., for rotational energies E_r less than ~ 40 kJ/mol) but actively promotes reactivity at higher energies. Molecular vibrational energy E_v is found to be only half as efficacious as E_n in promoting dissociation. Finally, phonons are able to provide additional energy from the surface, E_s , to help overcome the ~ 60 kJ/mol activation barrier for hydrogen dissociative chemisorption when molecular energy is in short supply.¹⁴ The MURT, with molecular rotations and parallel translation treated as spectator

* Author to whom correspondence should be addressed. E-mail: harrison@virginia.edu.

degrees of freedom, is able to provide a remarkably^{10,15–17} quantitative accounting of the H₂/Cu(111) reactivity, characterize the transition state, and provide a statistical baseline for the gas–surface reactivity against which dynamical effects can be identified.

Key experimental inferences for H₂/Cu(111) that run contrary to some popularly held theoretical notions are that (i) surface phonons^{10,18} play a vital role in the hydrogen chemisorption dynamics, (ii) molecular rotations^{16,19} are approximately spectator degrees of freedom at thermally accessible energies, and (iii) the transition state for dissociative chemisorption is early rather than late.²⁰ These conclusions are defensible based on the existent experimental data alone but are bolstered by the MURT modeling of this report.

Earlier MURT analysis of the activated dissociative chemisorption of hydrogen,¹⁷ silane,²¹ methane,^{6,7,22–24} and ethane²⁵ on various surfaces did not treat molecular rotation as a spectator but rather assumed that rotational energy actively promotes reactivity. When a MURT model was recently applied to dissociative chemisorption of hydrogen on Cu(111) with rotation fully participatory in the reaction dynamics,¹⁷ simulations of the same experimental data as treated here were oftentimes markedly different. For example, with participatory rotations, the experimental behavior at high rotational quantum numbers $J > 6$ and rotational energies $E_r > 30$ kJ/mol is well reproduced by the MURT, but the low- J behavior is not. To allow for a complete and direct comparison between the MURT simulations with rotation included and excluded from participation in the hydrogen dissociation dynamics, the figures of the current paper are formatted quite similarly to those of its predecessor. The spectator approximation holds well at thermally accessible rotational energies (i.e., $E_r < 40$ kJ/mol) and leads to calculated thermal associative desorption angular yields and energy distributions, in addition to thermal dissociative sticking coefficients, S_T , that are in improved agreement with experiment. Order of magnitude variations in S_T are calculated depending on whether rotation is treated as active¹⁷ or inactive in the dissociation dynamics. Consequently, establishing the role of rotation in dissociative chemisorption is shown to be of considerable importance for accurate theoretical simulations. There is some evidence that rotation is also approximately a spectator in the activated dissociative chemisorption of CO₂ on Rh(111) and, by detailed balance, in the oxidation of CO on Rh(111).²⁶ Unfortunately, there are few experimental studies of gas–surface reactivity that resolve the role of rotation.

Given that many key industrial processes can be rate-limited by activated dissociative chemisorption, such as H₂ production by CH₄ reforming on Ni catalysts²⁷ or SiH₄ chemical vapor deposition of Si on Si(100) in microelectronics fabrication,²⁸ developing an improved molecular-level understanding of dissociative sticking is desirable.¹⁸ This paper allows for a ready assessment of the capabilities and limitations of the statistical MURT model through its simulation of the gas–surface reactivity of the H₂/Cu(111) benchmark system.

II. Physisorbed Complex Microcanonical Unimolecular Rate Theory.

The physisorbed complex (PC) MURT local hot spot model^{6,22,23} applied to the H₂/Cu(111) dissociative chemisorption kinetics is schematically depicted in Figure 1 and is described microcanonically as

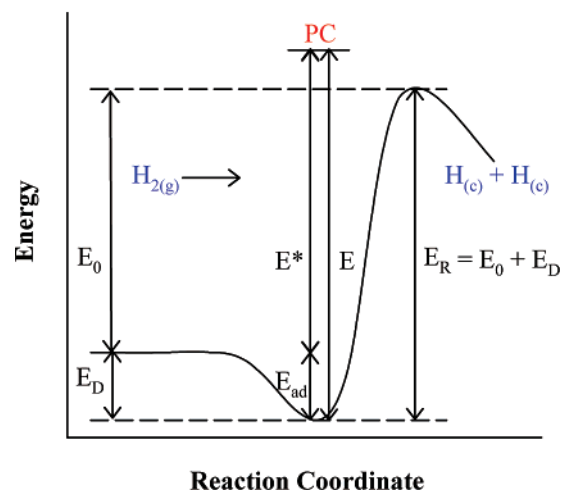
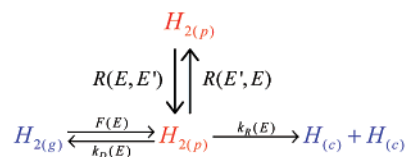
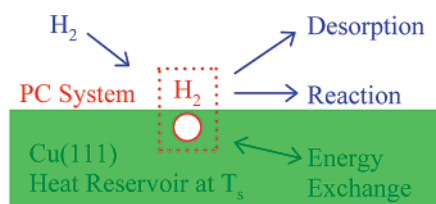
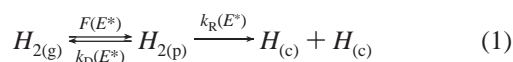


Figure 1. Schematic depiction of the kinetics and energetics for the activated dissociation of H₂ on Cu(111). Surface coordination numbers have been suppressed in the kinetic equations, and the zero-point energies are implicitly included in the two-dimensional potential energy curve along the reaction coordinate. Energy transfer rates $R(E', E)$ between the PCs and surrounding surface heat bath are assumed to be negligible given ultrafast H₂ desorption rates at reactive energies, obviating the need for a more complicated Master Equation approach.^{22–24}

Hydrogen incident on the surface forms a transient gas–surface collision complex consisting of the molecule and a few adjacent surface atoms represented as s surface oscillators that vibrate at the mean Cu phonon frequency. This local hot spot is an energetic, transient intermediate species, which is not in thermal equilibrium with the remainder of the substrate. Energy in this transiently formed physisorbed complex (PC or H_{2(p)} in eq 1) is assumed to be microcanonically randomized in an ensemble-averaged sense through the collision process itself²⁹ and/or rapid intramolecular vibrational energy redistribution.²² Molecular translation parallel to the surface and rotations are treated as spectators to the H₂/Cu(111) chemisorption dynamics based on experimental observations. The active exchangeable energy E^* ($= E_n + E_v + E_s$) of the PC in eq 1 and Figure 1 has its zero at $T = 0$ K with the molecule and surface infinitely apart. PCs formed with total energy E^* at flux rate $F(E^*)$ competitively desorb or react with RRKM rate constants $k_D(E^*)$ and $k_R(E^*)$, respectively. Ultrafast molecular desorption rates at the elevated PC energies sufficient for reaction (i.e., activated dissociative chemisorption) are presumed to severely limit energy exchange between the PCs and the surrounding metal. Consequently, PCs formed at energies sufficient for reaction can be treated microcanonically as approximately adiabatically isolated systems over their short lifetimes.

Applying the steady-state approximation to the H_{2(p)} coverage of eq 1 yields an expression for the initial dissociative sticking coefficient that is measured experimentally

$$S = \int_0^{\infty} S(E^*)f(E^*) dE^* \quad (2)$$

where

$$S(E^*) = \frac{W_R^\ddagger(E^* - E_0)}{W_R^\ddagger(E^* - E_0) + W_D^\ddagger(E^*)} \quad (3)$$

is the microcanonical sticking coefficient, W_D^\ddagger and W_R^\ddagger are the sums of state at the transition state for desorption and reaction, respectively, E_0 is the apparent threshold energy for the dissociative chemisorption, and

$$f(E^*) = \int_0^{E^*} f_n(E_n) \int_0^{E^* - E_n} f_v(E_v) f_s(E^* - E_n - E_v) dE_v dE_n \quad (4)$$

is the flux distribution for creating a PC at E^* . The $f(E^*)$ results from the convolution over the individual energy distribution functions for each degree of freedom that can actively exchange energy in the PC and thereby contribute energy toward surmounting E_0 . These individual energy distributions include the flux-weighted normal translational energy distribution $f_n(E_n)$ and vibrational energy distribution $f_v(E_v)$ of the incident hydrogen along with the surface energy distribution $f_s(E_s)$ for s surface oscillators vibrating at the mean Cu phonon frequency, $\nu_s = (3/4)k_B\theta_{\text{Debye}}/h$, of 175 cm⁻¹. The $W_D^\ddagger(E^*)$ sum of states in eq 3 is fixed by assuming translation along the surface normal is the reaction coordinate for desorption and the desorption transition state occurs with the molecule far from the surface with its gas-phase vibrational frequency fully developed. The reactive transition state for dissociative chemisorption is characterized by three parameters that are optimized through simulation of selected experiments by minimizing the average relative discrepancy (ARD) between the theory and the experiments, e.g., for sticking

$$\text{ARD} = \left\langle \frac{|S_{\text{theory}} - S_{\text{expt}}|}{\min(S_{\text{theory}}, S_{\text{expt}})} \right\rangle \quad (5)$$

The three reactive transition state parameters are the threshold energy for dissociative chemisorption, E_0 , the frequency of the vibrational mode perpendicular to the reaction coordinate in the transition state, ν_D , and the number of surface oscillators involved in the PC, s . The H–H vibrational mode is taken to be the reaction coordinate for dissociative chemisorption, and so ν_D roughly characterizes the vibration of the molecule against the surface along the direction of the surface normal at the reaction transition state, a mode that has evolved from normal translational motion of the free molecule toward the surface. To investigate if the reaction coordinate for dissociation was some other admixture of normal translation toward the surface and intramolecular stretching, the frequency range from 0 to 4500 cm⁻¹ for ν_D was considered, but high-frequency ν_D values did not yield good simulations of experiments. The Beyer–Swinehart–Stein–Rabinovitch³⁰ algorithm was used to calculate the sums and densities of states required in eqs 3 and 4 using the known anharmonicities for the hydrogen stretching vibration and assuming the ν_D and ν_s modes are harmonic.

A strength of the MURT formalism is that, once the reactive transition state characteristics have been defined by fits to

experiments or in principle by electronic structure calculations, the dependence of an experimental sticking coefficient on any dynamical variable (T_s , E_i , E_v , etc.) can be simulated on the basis of eq 2 by averaging the microcanonical sticking coefficient over the probability for creating a PC at E^* under the specific experimental conditions of interest. The principle of detailed balance at thermal equilibrium allows the dynamics of the thermally driven associative desorption of hydrogen to be calculated given knowledge (or simulation) of state-resolved thermal dissociative sticking coefficients. Conversely, thermal associative desorption experiments are able to explore the roles of molecular vibrational, rotational, and translational (E_v , E_r , and E_t) energies on the dissociative sticking via the principle of detailed balance.¹¹ Detailed balance asserts that the thermal associatively desorbing hydrogen flux should exactly balance the flux of hydrogen that would successfully dissociatively stick under thermal equilibrium conditions, even at quantum-state-resolved levels of detail. In this way, studies of associative desorption can provide detailed information about the reverse process, dissociative sticking, that occurs over the same PES.

The three dissociative chemisorption transition state parameters required by the MURT were fixed by optimizing the simulation of all of the available thermally driven associative desorption experiments^{11–14} for both H₂ and D₂ of the kind illustrated in Figures 3, 5, and 6b below. The resulting optimal parameter set $\{E_0 = 62 \text{ kJ/mol}, \nu_D = 490 \text{ cm}^{-1}, s = 1\}$ for H₂/Cu(111) was maintained throughout all of the calculations and figures in this report unless explicitly noted otherwise (standard zero-point and mass-based frequency corrections were applied for D₂/Cu(111)). DFT calculations of a six-dimensional (6D) reactive PES for H₂/Cu(111) predict fairly similar transition state characteristics: $E_0 \approx 48 \text{ kJ/mol}$ and frustrated rotations and translations in the range of $405 \text{ cm}^{-1} \leq \nu_i \leq 1050 \text{ cm}^{-1}$.^{20,31,32} DFT calculations in 2006 defining a 6D PES for the presumably more reactive H₂/Cu(110) system gave $E_0 = 58 \text{ kJ/mol}$,¹⁹ a value that might also stand as the current DFT lower bound estimate for H₂/Cu(111).

III. Results and Discussion

A. Internal State-Averaged Dissociative Sticking and Associative Desorption. Molecular beam studies of hydrogen dissociative chemisorption on Cu(111) have measured nonequilibrium dissociative sticking coefficients,^{11,12} and in simulating these experiments (as depicted in Figure 2) it was assumed that the molecular beam nozzle temperature T_n sets the vibrational temperature of the beam molecules as $T_v = T_n$ as was estimated experimentally.¹¹ The sticking calculated by the PC-MURT is in qualitative agreement with the experiments performed by the IBM Research Division,^{11,12} but the fall off in sticking as T_n is reduced is not as marked as seen experimentally, particularly at low E_n . Similar H₂/Cu(111) molecular beam experiments by Rendulic and co-workers³³ at $T_n = 1200 \text{ K}$ and $T_s = 190 \text{ K}$ gave sticking coefficients 1–2 orders of magnitude higher than the IBM experiments at $T_n = 1235 \text{ K}$. The cause of this discrepancy between experiments is unknown. Assurance that the IBM sticking coefficients are consistent with at least some other experimental data comes from the demonstration that the IBM dissociative sticking coefficients can be reproduced by detailed balance with parameters close to those derived from related thermal associative desorption experiments given some assumptions about the surface temperature dependence of the dissociative sticking dynamics.¹¹

Figure 3 shows the angular distribution of associatively desorbing D₂ that peaks around the surface normal and broadens

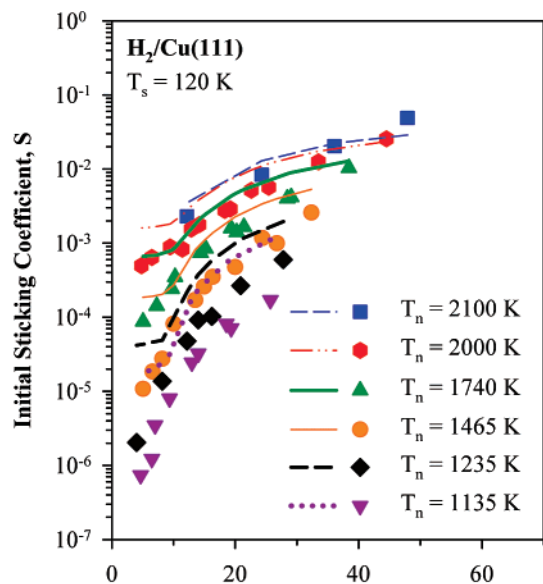
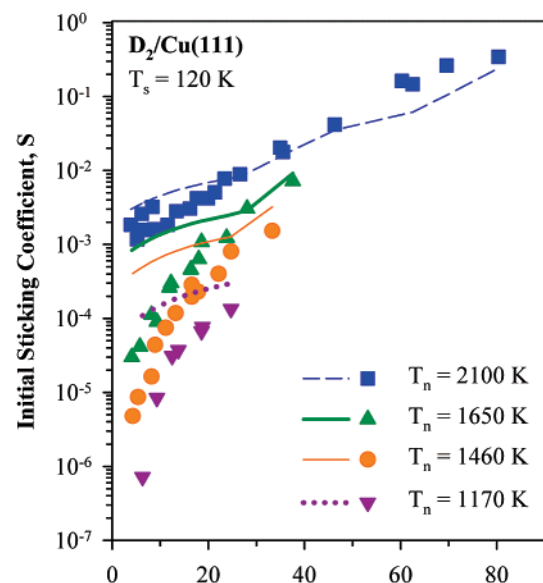
(a) Normal Translational Energy, E_n [kJ/mol](b) Normal Translational Energy, E_n [kJ/mol]

Figure 2. Absolute dissociative sticking coefficients for thermally populated molecular beams^{11,12} of (a) H_2 and (b) D_2 at specified nozzle temperatures (points) in comparison to PC-MURT simulations (lines).

as the surface temperature is increased. The PC-MURT slightly underpredicts the ~ 60 kJ/mol $\langle E_i \rangle$ of desorbing D_2 near the surface normal ($E_0(D_2) = 69$ kJ/mol) but recovers the asymptotically correct $\langle E_i \rangle \rightarrow 2k_B T_s$ as $\vartheta \rightarrow 90^\circ$ for a reactive system obeying normal translational energy scaling, unlike the one-dimensional (1D) van Willigen³⁴ and five-dimensional (5D) quantum scattering calculations.³⁵ Although the 1D van Willigen model with $E_0 = 24$ kJ/mol can reproduce the angular distributions of Figure 3a very well with an ARD of just 23%,¹⁷ its catastrophe that $\langle E_i \rangle \rightarrow \infty$ as $\vartheta \rightarrow 90^\circ$ points to the kind of nonphysicality that can be introduced when severely reduced dimensionality models are employed to describe inherently multidimensional reaction dynamics.

B. Eigenstate-Resolved Dissociative Sticking and Associative Desorption. B.1. Role of Rotation. Figure 4 shows vibrationally resolved $\langle E_i \rangle$ and rotational distributions for associatively desorbing hydrogen as functions of the rotational

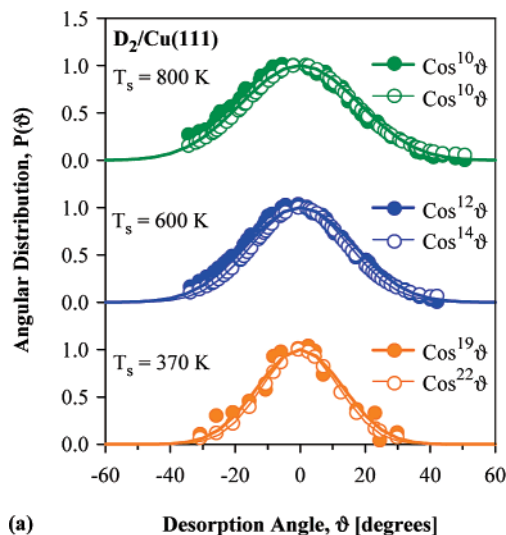
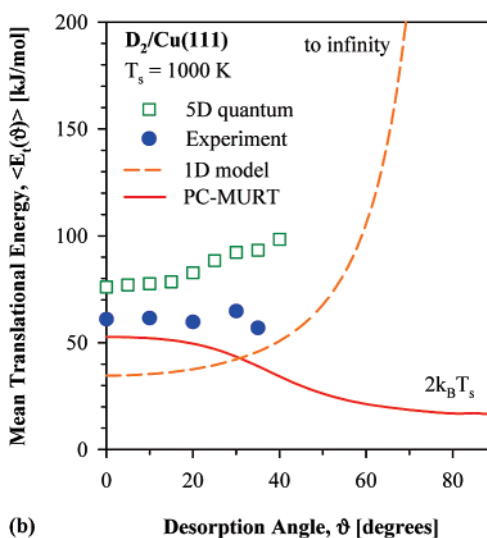
(a) Desorption Angle, ϑ [degrees](b) Desorption Angle, ϑ [degrees]

Figure 3. (a) Experimental^{11,12} (solid points and bold lines) and PC-MURT (open points and thin lines) angular distributions and $\cos^n \vartheta$ fits for D_2 associative desorption from Cu(111) at various surface temperatures. (b) Experimental mean translational energies for associative desorption as a function of angle¹³ (solid points) in comparison to those calculated by a 5D quantum scattering model³⁵ (open points), van Willigen model³⁴ (dashed line), and the PC-MURT (solid line).

quantum number J and the rotational energy E_r . Experimental rovibrational probabilities $P_{\nu,J}$ were normalized by asserting they summed to one over the ν, J range of the measured eigenstates. The PC-MURT $P_{\nu,J}$ values sum to 1.000 over the theoretically considered $\nu = 0-5$ and $J = 0-26$ ranges of eigenstates and sum to 0.999 over the more limited experimental range of measured eigenstates. The PC-MURT rotational distributions are necessarily Boltzmann at the surface temperature, $P_{\nu,J} \propto g_n(2J+1) \exp(-E_r/k_B T_r)$ where $T_r = T_s$ and g_n is the nuclear spin degeneracy, because rotation is treated as a spectator degree of freedom. The PC-MURT predicts the eigenstate-resolved experimental data quite well, particularly for the lower vibrational and rotational states that are most heavily weighted in thermal sticking calculations. The increasing divergence of the experimental data from PC-MURT simulations for $J \geq 7$ ($E_r \geq 39$ kJ/mol) for H_2 and $J \geq 10$ ($E_r \geq 38$ kJ/mol) for D_2 is indicative of an increasing breakdown of rotation's spectator status at these high rotational energies that are relatively thermally inaccessible at the experimental temperature of 925 K where $k_B T_s = 7.7$ kJ/mol. Earlier MURT modeling of H_2 /Cu(111) assuming that rotational energy was fully participatory

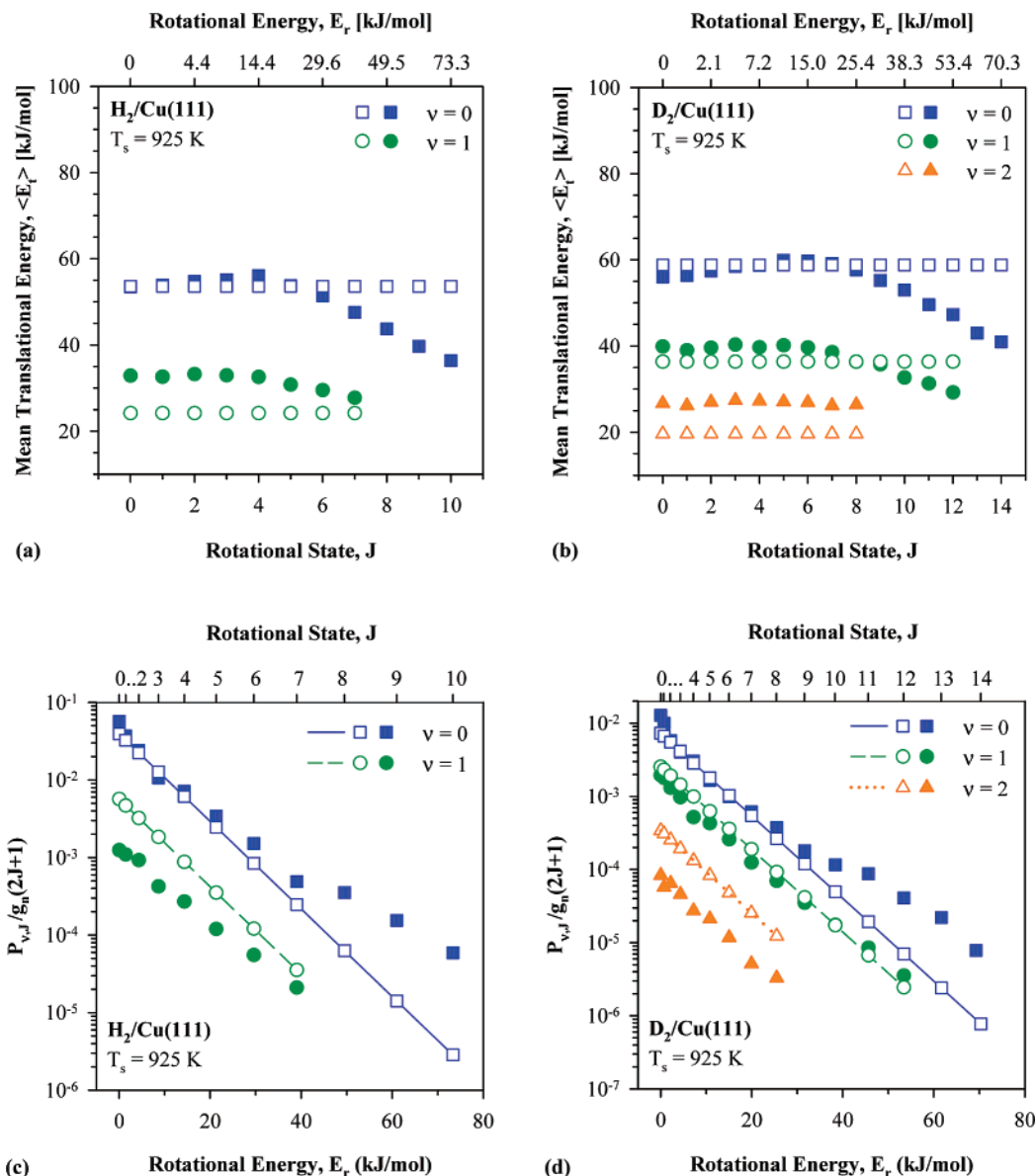


Figure 4. (a and b) Experimental^{11,12} (solid points) and PC-MURT (open points) mean translational energies as a function of rovibrational state for associatively desorbing hydrogen. (c and d) Experimental^{11,12} (solid points) and PC-MURT (open points) rotational energy distributions for hydrogen associative desorption in various vibrational states in Boltzmann plots. Lines through the PC-MURT rotational distributions are Boltzmann distributions with rotational temperature equal to the surface temperature.

in promoting dissociation predicts that $\langle E_t \rangle$ in Figures 4a and 4b should fall monotonically with increasing J and that the rotational temperatures of Figures 4c and 4d should lie in the range from $T_r = 6411$ to 2399 K (i.e., so the slopes of the rotational Boltzmann plots should be far more shallow).¹⁷ Consequently, the experimental data of Figure 4 can be considered to represent a varying admixture of these limiting rotational behaviors with the breakdown of rotation's initially purely spectator status occurring at rotational energies near 40 kJ/mol.

Only if rotation is treated as a spectator to the hydrogen dissociative chemisorption does the MURT model gain quantitative agreement with most aspects of the diverse dissociative chemisorption/associative desorption experiments (i.e., Figures 3 and 4 at low J , Figures 6 and 8, but not so much Figures 2 and 5) and extract transition state parameters from experiments that are quite close to the expectations of DFT calculations.^{20,31} The earlier two-parameter PC-MURT analysis¹⁷ that assumed fully participatory rotation and employed DFT-calculated frequencies for the dissociative transition state required a

considerably higher threshold energy for dissociative chemisorption (cf. $E_0 = 79$ vs 62 kJ/mol) to achieve its optimal, but more limited, agreement with experiments. The finding that the experiments are well-modeled with rotation as a spectator, at least until rotational energies of ~ 40 kJ/mol are exceeded, implies that the net effects of dynamical steering and reactive stereodynamics³⁶ for this reaction are negligible at thermally accessible energies.

Apart from any theoretical model, the low- J (i.e., $E_r \leq 40$ kJ/mol) associative desorption experimental data of Figure 4 are by themselves consistent with rotation being a spectator degree of freedom. There is arguably negligible variation of the $\langle E_t \rangle$ of the desorbing molecules over these J in Figures 4a and 4b, and the Boltzmann plots of Figures 4c and 4d have rotational temperatures equal to the surface temperature. By detailed balance, at thermal equilibrium this means that (i) even though increasing rotational energy of the incident molecules is made available with increasing J the $\langle E_t \rangle$ of the successfully reacting molecules does not change appreciably, even when E_r reaches ~ 40 kJ/mol, which is a substantial fraction of the

reaction threshold energy $E_0 = 62$ kJ/mol, and (ii) of the molecules incident on the surface at equilibrium with rotational temperature, $T_r = T_s = T$, the successfully reacting molecules have the same rotational temperature as all of the incident molecules, $T_r = T_s$, so there is no preferential reactivity from rotationally hotter molecules. At higher J and $E_r > 40$ kJ/mol, the experiments argue for rotation beginning to play an active role in the chemisorption dynamics. Fairly suddenly, the $\langle E_t \rangle$ of the successfully reacting molecules begins to fall monotonically with increasing J in Figures 4a and 4b, and the rotational temperatures extractable from the Boltzmann plots of Figures 4c and 4d at high J are much hotter than the 925 K surface temperature (i.e., $T_r = 1906$ K for $\text{H}_2(v=0)$ and 1540 K for $\text{D}_2(v=0)$). For these high- J states, detailed balance indicates that rotational energy is increasingly used to help surmount E_0 and thereby lower the $\langle E_t \rangle$ requirement for reaction. Rotational temperatures higher than T_s argue for preferential reactivity of molecules that are rotationally hotter than the thermal distribution of molecules at $T_r = T_s = T$ incident on the surface at thermal equilibrium. Consistent with the interpretations above, the PC-MURT with rotation as a spectator is able to explain and simulate the low- J experiments, and a PC-MURT model with fully participatory rotation¹⁷ is able to largely explain and simulate the high- J experiments. Why and how there is a crossover between these limiting behaviors near $E_r \approx 40$ kJ/mol is not clear.

Rettner and co-workers pointed out that the modest but discernible rise and then fall of $\langle E_t \rangle$ with J in their Figures 4a and 4b data is consistent with rotational motion initially hindering and then promoting dissociative chemisorption with increasing J . This led to considerable excitement about the possible role of steering and steric effects in the gas-surface reaction dynamics,^{36–39} particularly when a 6D quantum dynamics study⁴⁰ reported these effects to be important for dissociative chemisorption of H_2 on Pd(111). If broadside attack of the hydrogen on a metal is most favorable for reaction, then by detailed balance the molecules should leave the surface with this same preferential alignment. If the PES tends to steer incoming molecules into the most favorable alignment for dissociative sticking, then by detailed balance the preferential alignment of the nascent desorbing molecules should be scrambled by the PES during their exit from the near-surface region. Eigenstate-resolved measurements of the rotational polarization³⁷ of associatively desorbing D_2 from Cu(111) found that the molecules were unpolarized for $J = 0$, less than 10% preferentially polarized as helicopters (molecules rotating in the plane parallel to the surface) for $J \leq 5$ ($E_r \leq 11$ kJ/mol), and less than 20% for $J \leq 10$ ($E_r \leq 38$ kJ/mol). The rather modest polarization at low J might be attributable to steering, but it is also in rough accord with the prediction of random polarization by the PC-MURT and a recent classical trajectory study¹⁶ on a 6D PES. For $J \geq 6$, where rotation begins to enhance dissociative chemisorption, Auerbach, Wodtke, and co-workers³⁶ observed that the polarization of the desorbing molecules increases as E_t is reduced, which is consistent with the increasing steric preference of the successfully chemisorbing molecules for broadside attack as E_t is reduced. Steering, if present, should increase as E_t is reduced, and so, by detailed balance, the polarization of desorbing molecules should decrease as E_t is reduced (i.e., opposite to the observed trend). Consequently, steering is not believed to play a significant role in the $\text{H}_2/\text{Cu}(111)$ reactivity.³⁶

B.2. Dynamical Bias toward Normal Translation over Vibration: Early Barrier. Summing over the rotational states of

TABLE 1: Vibrational Distributions for Associative Desorption from Figures 4c and 4d

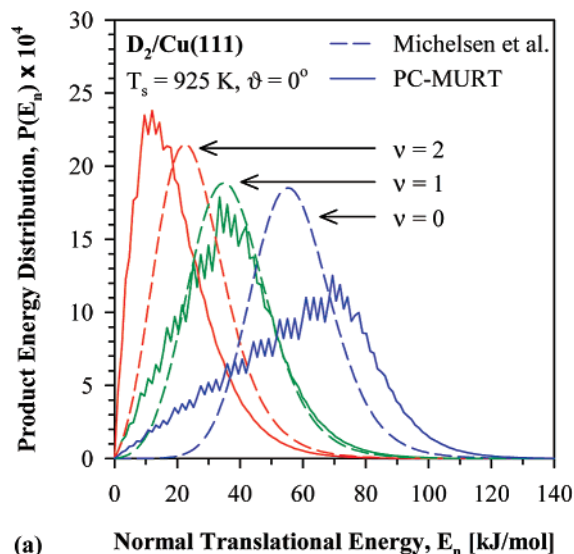
	ν	J sum	$P_\nu(\text{expt.})$	$P_\nu(\text{MURT})$
H_2	0	0–10	96.7%	90.9%
	1	0–7	3.3%	9.0%
	$\Sigma P_{\nu,J}$		100%	99.9%
D_2	0	0–14	82.4%	75.3%
	1	0–11	16.8%	22.7%
	2	0–8	0.8%	1.9%
	$\Sigma P_{\nu,J}$		100%	99.9%

Figures 4c and 4d yields the product vibrational distributions for hydrogen associative desorption reported in Table 1. By detailed balance, the product flux distributions for associative desorption must equal the reactive flux distributions for dissociative chemisorption (i.e., $P_\nu(E_\nu) = S_\nu(E_\nu) f_{\text{MB}}(E_\nu)$). The MURT calculates somewhat more vibrational excitation than is experimentally observed. This is consistent with the MURT treating vibrational and normal translational energy as equally efficacious in promoting dissociative chemisorption whereas experiments¹¹ have established that vibrational energy is only half as efficacious as normal translational energy.

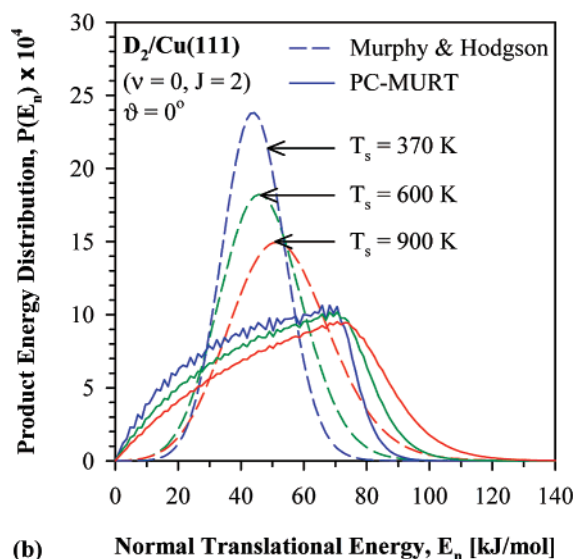
Rotationally averaged, vibrationally resolved normal translational energy distributions for D_2 associative desorption along the surface normal at $T_s = 925$ K are shown in Figure 5a. The PC-MURT reproduces the experimental distributions only qualitatively, seems to overemphasize the low E_n tails of the distributions, and likely chooses too high a value of E_0 (see high E_n edge for $\nu = 0$) as a compromise because it overestimates the vibrational efficacy. When averaged over all vibrational and rotational states of associatively desorbing hydrogen, the PC-MURT predicts somewhat less mean translational energy release than is observed experimentally in Figure 3b.

The PC-MURT is a statistical, microcanonical theory in which all forms of energy that contribute to the total active, exchangeable energy, $E^* = E_n + E_\nu + E_s$, are assumed to be equally effective in surmounting the threshold energy for dissociation. By comparison to the PC-MURT distributions, the measured associative desorption product state distributions show that the energy release from the transition state is not perfectly statistically distributed but rather there is a dynamical bias toward translational energy release and away from vibrational energy release. Via detailed balance, these observations indicate that translational energy is more effective in promoting dissociative chemisorption than vibrational energy.

Dynamical biases in gas-phase reaction dynamics have been extensively studied and codified in the Polanyi rules,⁴¹ which argue that if the $\text{H}_2/\text{Cu}(111)$ transition state is positioned early in the dissociative chemisorption entrance channel of the PES, then molecular translational energy should be favored over vibrational energy in promoting dissociation. Reduced dimensionality coupled cluster wave packet simulations and classical trajectory calculations on model potentials mimicking possible $\text{H}_2/\text{Cu}(111)$ PESs have been explored by Holloway and co-workers who found that the Polanyi rules should also apply to surface reaction dynamics.^{42,43} Problematic is that there is no ab initio full dimensionality (i.e., seven-dimensional (7D) or more) PES for the $\text{H}_2/\text{Cu}(111)$ system that is known to be chemically accurate. However, there is no need to invoke a late barrier for chemisorption to explain the product vibrational excitation in associative desorption because the dynamically unbiased, statistical PC-MURT already calculates a product vibrational distribution with more vibrational excitation than is experimentally observed. Interestingly, an early rather than late



(a)



(b)

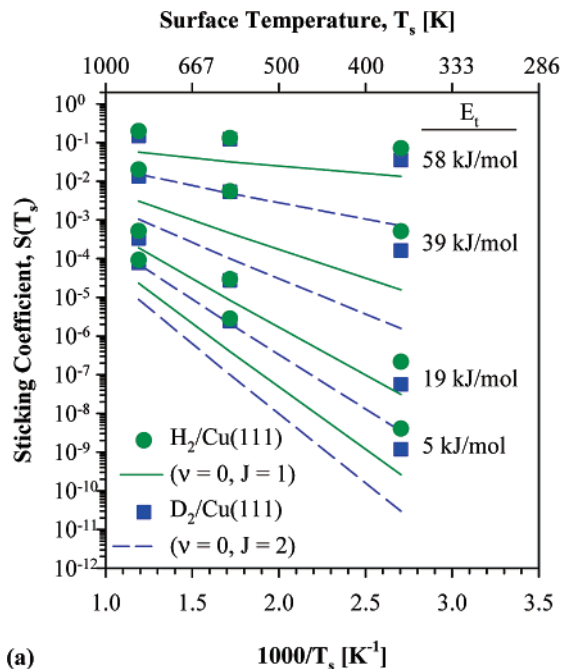
Figure 5. (a) Experimental¹² (dashed lines) and PC-MURT (solid lines), rotationally averaged from $J = 0$ to 6 and vibrationally resolved, translational energy distributions for associatively desorbing D₂. (b) Experimental¹⁴ (dashed lines) and PC-MURT (solid lines), rovibrational eigenstate-resolved translational energy distributions for associatively desorbing D₂ as a function of surface temperature.

transition state PES topology is consistent with local density approximation (LDA) rather than GGA-DFT calculations.²⁰ GGA-DFT calculations seem to invariably predict late transition states for activated dissociative chemisorption,⁴⁴ but the Polanyi rules applied to the measured hydrogen dissociative chemisorption dynamics suggest that this need not always be the case.

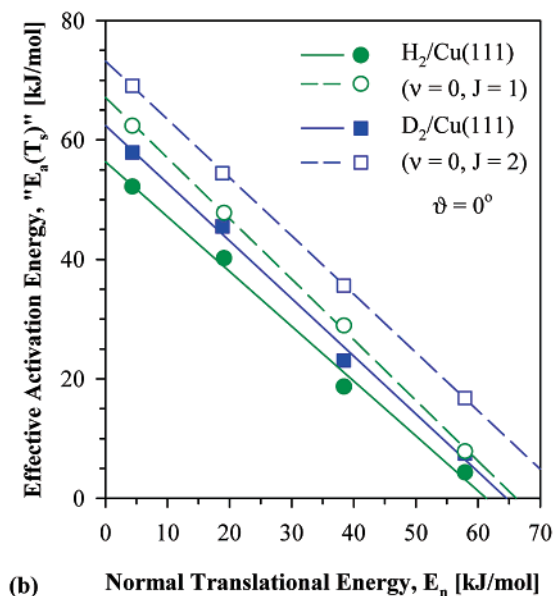
B.3. Role of the Surface. Figure 5b shows rovibrational eigenstate-resolved translational energy distributions $P(E_n, \vartheta = 0^\circ; \nu, J, T_s)$ from thermal associative desorption measured by Murphy and Hodgson¹⁴ as a function of T_s are only qualitatively simulated by the PC-MURT. Detailed balance allows these measurements to define relative eigenstate-resolved dissociative sticking coefficients according to

$$S(E_n, \vartheta = 0^\circ; \nu, J, T_s) \propto \frac{P(E_n, \vartheta = 0^\circ; \nu, J, T_s)}{f_{\text{MB}}(E_n, T_s)} \quad (6)$$

where $f_{\text{MB}}(E_n, T_s) \propto E_n \exp(-E_n/k_B T_s)$ is the flux-weighted Maxwell-Boltzmann distribution for molecular translational



(a)



(b)

Figure 6. (a) Surface temperature dependent, rovibrational eigenstate-resolved, relative dissociative sticking coefficients¹⁴ (solid points) obtained by detailed balance from the Figure 5b associative desorption experiments in comparison to absolute sticking coefficients simulated by the PC-MURT (lines). (b) Experimental¹⁴ (solid lines and points) and PC-MURT (dashed lines and open points) “effective” activation energies, “ $E_a(T_s)$ ” = $-k_B \partial \ln S / \partial T_s^{-1} = \langle E_s \rangle_R - \langle E_s \rangle$, for rovibrational eigenstate-resolved dissociative sticking coefficients as a function of normal translational energy.

energy at temperature T_s . Murphy and Hodgson normalized their relative $S(T_s)$ curves by assuming that they attain a common limiting value of 1 at high E_n . The $S(T_s)$ shows an Arrhenius T_s dependence that varies with E_n as illustrated in Figure 6. Figure 6a shows remarkable agreement between the relative sticking coefficients reported by Murphy and Hodgson and the absolute values calculated by the PC-MURT. Figure 6b also shows good agreement between experimental and PC-MURT values of the “effective” activation energies “ $E_a(T_s)$ ” = $-k_B \partial \ln S / \partial T_s^{-1}$ as a function of E_n . The nonequilibrium Tolman relation²² “ $E_a(T_s)$ ” = $\langle E_s \rangle_R - \langle E_s \rangle$ applies where $\langle E_s \rangle_R$ is the average energy derived from the surface for those PCs that successfully react (i.e.,

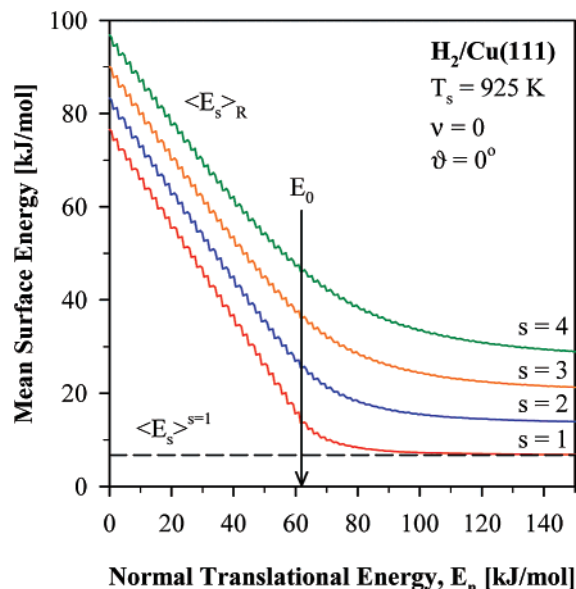


Figure 7. PC-MURT calculations of the mean surface energy of the successfully reacting PCs (solid lines) as a function of normal translational energy plotted for $s = 1$ –4 along with the mean surface energy for a single surface oscillator (dashed line) in molecular eigenstate-resolved dissociative sticking experiments.

dissociatively chemisorb) and $\langle E_s \rangle$ is the average energy derived from the surface for all PCs formed under the experimental conditions of interest. Because $\langle E_s \rangle_R > "E_a(T_s)"$, the experiments of Figure 6b make clear that more than 50 kJ/mol of energy from surface phonons can be used to help surmount the dissociative chemisorption barrier when molecular energy is in short supply. The PC-MURT analytically predicts $\partial "E_a(T_s)" / \partial E_n = \partial \langle E_s \rangle_R / \partial E_n = -1$ for $E_n < E_0 - E_v$ when rotation is a spectator and $s = 1$.¹⁷

B.3.1 Number of Surface Oscillators. Of interest because $\partial "E_a(T_s)" / \partial E_n = \partial \langle E_s \rangle_R / \partial E_n$ is experimentally observable, Figure 7 plots the PC-MURT-calculated $\langle E_s \rangle_R$ as a function of normal translational energy and number of surface oscillators in the PCs. When E_n is between 0 and E_0 , the slope $\partial \langle E_s \rangle_R / \partial E_n$ is -1 for a single surface oscillator and becomes shallower as the number of surface oscillators increases. For example, $s = 2, 3$, and 4 correspond to slopes of $-0.93, -0.87$, and -0.82 , respectively. Consequently, the equivalent $\partial "E_a(T_s)" / \partial E_n$ slopes of Figure 6b derived from Murphy and Hodgson's experiments and analysis¹⁴ are consistent with $s \approx 2 \pm 1$ (the PC-MURT overall optimized value of s is 1). The Murphy and Hodgson type of experiments may prove generally useful in helping to determine the number of surface oscillators in other activated dissociative chemisorption systems. For any number of surface oscillators, $\langle E_s \rangle_R$ asymptotically approaches the mean surface energy $\langle E_s \rangle$ as E_n exceeds E_0 but more slowly with increasing s as can be seen in Figure 7. In the high-temperature equipartition limit reached at 925 K, the mean surface energy of s Planck vibrational oscillators⁴⁵ is $\langle E_s \rangle = s(k_B T_s - hv_s/2)$. Figure 7 indicates that the effective activation energy " $E_a(T_s)" = \langle E_s \rangle_R - \langle E_s \rangle$ of Figure 6b will tend to zero rather than become negative in the high E_n limit.

C. Dissociative Sticking at Thermal Equilibrium and with Effusive Beams. Although direct measurements of the thermal equilibrium dissociative sticking of hydrogen on Cu(111) are lacking, Rettner and co-workers⁴⁶ provide an experimentally derived estimate of the 925 K thermal dissociative sticking coefficient of D_2 on Cu(111) as $S_T(925 \text{ K}) = 3.3 \times 10^{-4}$ based on detailed balance analysis of their 925 K eigenstate-resolved

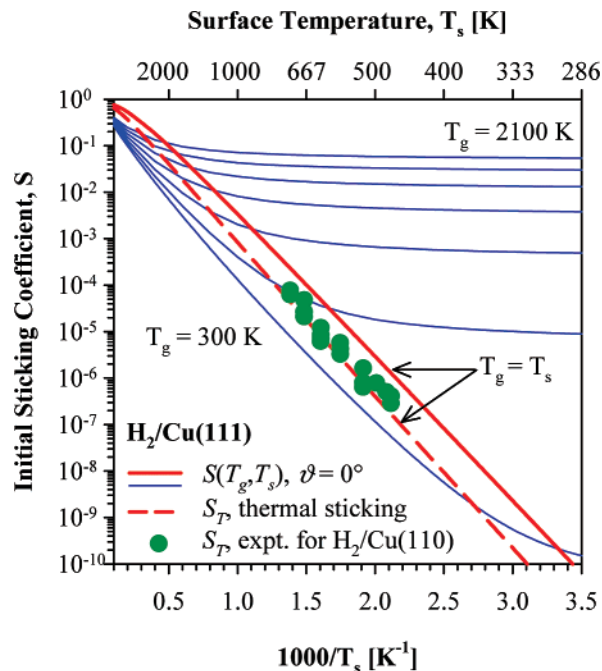


Figure 8. PC-MURT simulation of the thermal equilibrium dissociative sticking coefficient, S_T , given by the dashed bold line. Experimental measurements (solid points) of S_T for H_2 on Cu(110) taken at 47 and 78 Torr⁴⁷ are shown for comparison because no recent direct experimental measurements of S_T are available for H_2 /Cu(111). PC-MURT predictions for the dissociative sticking coefficient, $S(T_g, T_s)$, of an effusive beam of H_2 gas incident along the surface normal are given as a function of T_g and T_s (solid lines). The thin lines are for $T_g = 300$ –2100 K in 300 K increments, while the bold line is for $T_g = T_s$.

associative desorption experiments. Their calculations required defining over 100 semiempirical parameters from experiments, three parameters to describe the translational energy distribution for each rovibrational eigenstate displayed in Figure 4. The three-parameter MURT predicts $S_T(925 \text{ K}) = 2.2 \times 10^{-4}$ for D_2 on Cu(111), just 33% less than the experimentally based estimate. Figure 8 shows that the H_2 /Cu(111) thermal dissociative sticking coefficient calculated by the PC-MURT is well-described by an Arrhenius expression, $S_T = S_0 \exp(-E_a/k_B T)$ where $S_0 = 1.57$ and $E_a = 62.9 \text{ kJ/mol}$ over the temperature range $300 \text{ K} \leq T \leq 1000 \text{ K}$. At sufficiently high T , the calculated S_T deviates from Arrhenius behavior and rolls over toward a limiting value of 1. Figure 8 shows that the PC-MURT prediction of S_T for H_2 /Cu(111) is in good accord with experimental measurements for the H_2 /Cu(110) system.⁴⁷ Unfortunately, there are no modern direct experimental measurements of S_T for the H_2 /Cu(111) system.

Figure 8 also predicts nonequilibrium dissociative sticking coefficients, $S(T_g, T_s)$, for H_2 /Cu(111) appropriate to a thermal effusive beam at temperature T_g striking the surface at temperature T_s along the direction of the surface normal, which might be possible to measure experimentally at low pressures where T_g can be varied independent of T_s . Effusive beam experiments of this kind⁷ were recently completed for CH_4 dissociative chemisorption on Pt(111) and analyzed by the PC-MURT. Perhaps, Figure 8 may stimulate similar experiments for H_2 /Cu(111) dissociative chemisorption.

Table 2 compares the thermal sticking coefficient and Arrhenius parameters for H_2 /Cu(111), predicted with rotation as a spectator and with rotation as fully active in the chemisorption dynamics, with best-fit experimental values for H_2 /Cu(110). The experimentally reported thermal activation energy for the presumably more reactive H_2 /Cu(110) system⁴⁷ is $E_a =$

TABLE 2: Arrhenius Parameters Determined by a Least-Squares Fit of the PC-MURT and Experimental Thermal Dissociative Sticking Coefficients

surface	rotation	S_0	E_a (kJ/mol)	$S_T(600\text{ K})$	$S_T/S_{T,\text{spec}}$ at 600 K
Cu(111)	spectator	1.57	62.9	5.09×10^{-6}	1.00
	active ¹⁷	1.37	79.6	1.61×10^{-7}	$1/31.6$
Cu(110)	experiment ⁴⁷	1.11	59.6	7.14×10^{-6}	1.40

59.8 ± 5.9 kJ/mol. Important to point out is that the PC-MURT calculation of $S_T(600\text{ K})$ for H₂/Cu(111) with rotation as a spectator is 32-fold higher than the calculation with fully active rotation.¹⁷ An order of magnitude change in the thermal sticking coefficient, dependent on whether rotation is recognized to be a spectator degree of freedom or not, is significant and points to the value of dynamical experiments. Although the PC-MURT with active rotations¹⁷ can reproduce the angular distributions and mean translational energy for associatively desorbing hydrogen quite well, it fails to reproduce the experimental behavior of the thermally most populated low- J states, and this dooms its ability to accurately calculate the thermal sticking. The PC-MURT with rotation as a spectator has no such problem. An open question is whether rotational motion can commonly be approximated as a spectator to dissociative chemisorption in systems other than H₂/Cu(111).

The relative contributions that energy from different degrees of freedom make toward surmounting the activation barrier for dissociative chemisorption can be quantified by defining fractional energy uptakes²² as $f_i = \langle E_i \rangle_R / \langle E^* \rangle_R$, or the mean energy derived from the i th reactant degree of freedom for those PCs that successfully react divided by the mean energy of the successfully reacting PCs. These uptakes vary only slowly with temperature for the thermal dissociative sticking of H₂ near 500 K where the MURT predicts $f_n = 43\%$, $f_s = 41\%$ and $f_v = 16\%$ as can be seen in Figure 9. Contributing more than 40% of the energy to overcome the activation barrier, surface phonons play a vital role in the thermal dissociative chemisorption. Consequently, the surface should not generally be discounted in the theoretical modeling of H₂ chemisorption, as is common practice in current state-of-the-art 6D dynamical calculations.^{10,18}

D. Comparison with Previous Theoretical Modeling and Interpretation of Experiments. The PC-MURT model's three transition state parameters were optimized and defined by minimizing the ARD between theoretical simulations and experiments^{11–14} of the kind illustrated in Figures 3, 5, and 6b. The ability of the PC-MURT to harness the information content of this limited set of experiments to make the simulations embodied within Figures 2, 4, 6a, and 8 that are in quite good agreement with experiments is heartening. Although this implementation of the PC-MURT model treats both parallel translational energy and rotational energy as spectator degrees of freedom, it effectively treats the H₂/Cu(111) chemisorption dynamics at a 7D (6D molecular + 1D surface) level and can make specific predictions for even fully eigenstate-resolved dissociative sticking coefficients, $S(E_t, \vartheta; \nu, J, m_J, T_s)$. With only one parameter more than an Arrhenius rate constant, the relatively crude PC-MURT model is able to reproduce and rationalize the diverse experimental behavior illustrated in Figures 2–6 and 8 remarkably well. Below, we contrast the PC-MURT model with some more complicated dynamical models whose connection to TST on a full dimensionality PES is usually less readily apparent.

D.1. Efficacies and Uptakes of Different Forms of Energy To Promote Dissociative Chemisorption. Quantum-state-resolved associative desorption and molecular beam dissociative

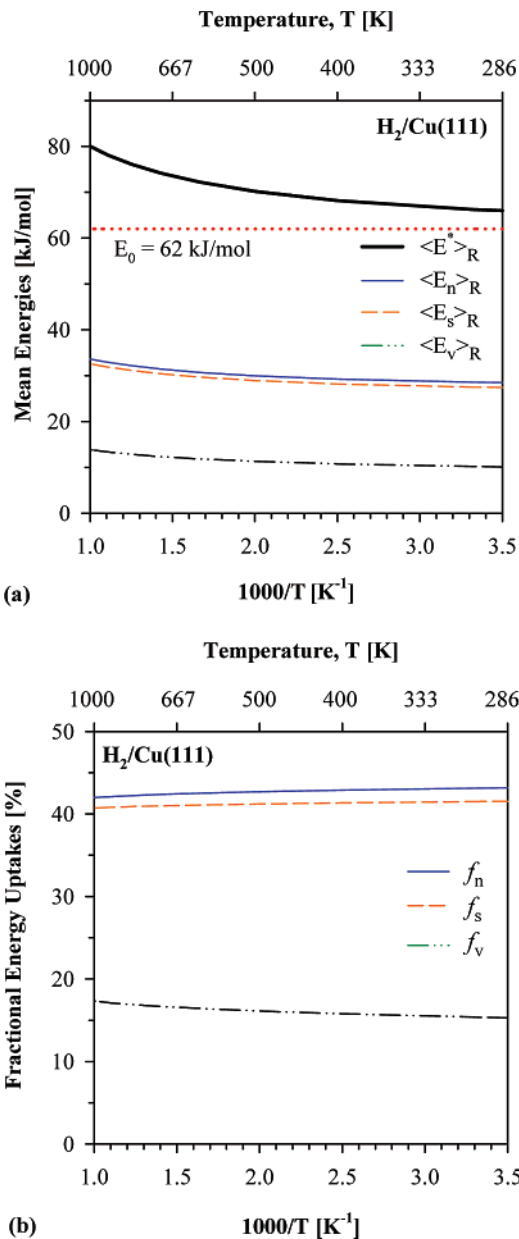


Figure 9. PC-MURT calculations of (a) the mean energies of the reacting physisorbed complexes that derive from different gas and surface degrees of freedom and (b) the fractional energy uptakes from the different degrees of freedom (e.g., $f_i = \langle E_i \rangle_R / \langle E^* \rangle_R$) for thermal dissociative sticking (averaged over all molecular angles of incidence).

sticking experiments^{11,12,14} have typically been analyzed in terms of the molecular eigenstate-resolved sticking coefficient obeying a semiempirically defined error function, erf, form⁴⁸

$$S(E_t, \vartheta; \nu, J, T_s) = \frac{A(\nu, J)}{2} \left[1 + \operatorname{erf} \left(\frac{E_c - \bar{E}_d(\nu, J)}{W(\nu, J; T_s)} \right) \right] \quad (7)$$

in which $A(\nu, J)$, $\bar{E}_d(\nu, J)$, and $W(\nu, J; T_s)$ are adjustable parameters. An effective translational energy is defined as

$$E_c = E_t \cos^n \vartheta \quad (8)$$

where n is an adjustable parameter. For the H₂/Cu(111) system, normal energy scaling is typically thought to approximately apply (i.e., $n = 2$), but $n = 1.8$ and $n = n(E_t)$ have been used in some instances to improve agreement with experiments.^{14,49} The $A(\nu, J)$ parameter is the limiting value of the sticking coefficient

at high E_e , $\bar{E}_d(v, J)$ is the value of E_e at the inflection point when the sticking has reached half its limiting value, and $W(v, J; T_s)$ is a width parameter that dictates the slope of the curve around its inflection point. The simplest model to motivate eq 7 is to assume that the impinging molecules dynamically sample a Gaussian distribution of energy barriers associated with molecular orientation and impact position across the surface unit cell and that passage over a particular barrier of energy E_b is a constant if $E_e > E_b$ and zero otherwise.^{50–52} Under this scenario, $\bar{E}_d(v, J)$ represents the mean dynamical barrier to dissociation for the (v, J) rovibrational state, and $W(v, J; T_s) = \sigma\sqrt{2}$ is defined by the standard deviation σ of the Gaussian distribution of barriers. Sticking coefficients of the eq 7 form have a sigmoid shape as a function of E_e . Interestingly, experimental^{53,54} and PC-MURT⁶ eigenstate-resolved dissociative sticking coefficients for vibrationally excited CH₄ impinging on metals also have a sigmoid shape that can be well fit by the eq 7 erf functional form.

Rettner and co-workers^{11,12} experimentally determined $\bar{E}_d(v, J = 0)$ values of 57.1 and 58.9 kJ/mol for H₂ and D₂, respectively. These values compare fairly closely to the reaction threshold energies of $E_0 = 62$ and 69 kJ/mol for H₂ and D₂, respectively, extracted by the PC-MURT. The vibrational efficacy for reaction was defined as

$$\xi_v = \frac{\bar{E}_d(v-1, J=0) - \bar{E}_d(v, J=0)}{E_v(v-1, J=0) - E_v(v, J=0)} = \frac{\Delta\bar{E}_d}{\Delta E_v} \quad (9)$$

to help characterize how effective vibrational energy was in lowering the translational energy requirement to surmount the mean dynamical barrier. Theoretically, one might prefer a vibrational efficacy definition of $[\partial S/\partial E_v]/[\partial S/\partial E_n]$ evaluated at given overall E^* , but eq 9 provides an experimentally measurable approximation. A value of $\xi_v = 0$ indicates that vibrational energy does not enhance reactivity. Rettner proposes that $\xi_v = 1$ indicates that vibrational energy is as effective as translational energy in promoting reaction (i.e., consistent with statistical theories). The experimentally derived $\bar{E}_d(v, J)$ values are numerically very similar to the rovibrationally resolved $\langle E_i \rangle$ values of Figure 4. For H₂ and D₂ on Cu(111),¹¹ experiments found that $\xi_v = 0.51 \pm 0.02$ for $v = 1$ and 2. At the lowest J , the rotational efficacy ξ_r , defined similarly to eq 9, is negative since $\bar{E}_d(v, J)$ increases slightly with J (cf. $\langle E_i \rangle$ in Figure 4). With increasing J , rotational efficacy increases through 0 until at $E_r > 20$ kJ/mol the rotational efficacy becomes positive and constant with values in the range of 0.25–0.48 dependent on vibrational state and isotope. In summary, experimental efficacy analysis based on the semiempirically defined $\bar{E}_d(v, J)$ parameters suggests that vibration is roughly 50% as effective as normal translational energy in promoting reaction whereas rotation can be inhibitory or a spectator at low J and is only about 25–50% as effective as translational energy at high J . On the face of these experimental inferences that normal translational energy is more efficacious than vibrational energy in promoting reaction, the Polanyi rules⁴¹ suggest that the dissociative transition state is early on the multidimensional PES so as to favor normal translational energy over vibrational energy.

The PC-MURT is a statistical theory, as can be seen from eq 3, which shows that the microcanonical sticking coefficient is simply the ratio of the number of open channels available for reaction over the total number of open channels to either react or desorb. The microcanonical theory assumes that all component forms of the active exchangeable energy $E^* = E_n + E_v + E_s$ are equally efficacious in promoting reaction. The

fractional energy uptakes $f_i = \langle E_i \rangle_R / \langle E^* \rangle_R$ predicted in Figure 9 describe the fraction of the average energy of the reacting PCs that derives from a particular degree of freedom under the thermal equilibrium conditions relevant to associative desorption/dissociative chemisorption detailed balance arguments. At the 925 K temperature of the Figure 4 associative desorption experiments, PC-MURT-calculated fractional energy uptakes are: $f_n = 42\%$, $f_s = 41\%$, $f_v = 17\%$, and $f_r = 0\%$. By detailed balance, the f_i 's are also the product fractional energy releases in the thermally driven associative desorption, or the fractions of the transition state energy $\langle E^* \rangle_R$ that go into the surface and molecular product energies, $\langle E_i \rangle_R$. Unlike the efficacy measures, which define the relative efficacy of one form of energy in promoting reaction over another, the fractional energy uptakes catalogue how efficiently different degrees of freedom serve as heat reservoirs to supply the activation energy necessary to thermally react. The availability of intramolecular vibrational energy ($\nu(\text{H}_2) = 4159 \text{ cm}^{-1}$) is much less than the availability of normal translational energy or surface phonon energy ($\nu_s = 175 \text{ cm}^{-1}$) given thermal Boltzmann energy distributions for the $f_i(E_i)$ distributions of eq 4, and this plays out in the fractional energy uptakes predicted by the PC-MURT.

The PC-MURT predicts that surface energy is about equally important as normal translational energy in surmounting the thermal activation energy, $E_a(T) = -k_B \partial \ln S_T / \partial T^{-1} = \langle E^* \rangle_R - \langle E^* \rangle$, at equilibrium (i.e., f_s/f_n is 98%). Murphy and Hodgson come to a similar conclusion regarding the efficacy of surface energy. They note that their measured low E_n , surface-temperature-dependent, effective activation energies " $E_a(T_s)$ " = $-k_B \partial \ln S / \partial T_s^{-1} = \langle E_s \rangle_R - \langle E_s \rangle$ of 52 and 58 kJ/mol for H₂ and D₂, respectively, are comparable to the mean dynamical barriers of 55 and 65 kJ/mol reported by Rettner and co-workers^{11,55} for the direct dissociative sticking of H₂ and D₂, respectively. PC-MURT simulations agree well with the Murphy and Hodgson experimental results as seen in Figure 6. Current state-of-the-art theoretical treatments of H₂ dissociative chemisorption¹⁰ and scattering¹⁸ on metals typically assume that the surface is a spectator to the gas–surface collision dynamics and treat only the molecular degrees of freedom in 6D calculations, an approach that has failed to quantitatively describe the H₂/Cu(111) reactivity.^{15,16,38,39} Lower-dimensional theoretical models^{56,57} aimed at capturing the surface temperature dependence of dissociative chemisorption have not yet proven capable of reproducing the Murphy and Hodgson experiments¹⁴ of Figures 5b and 6, nor have they been able to simultaneously reproduce the full range of experimentally observed behaviors illustrated in Figures 2–6 and 8 as well as the PC-MURT.

Let us return to consider the robustness and appropriateness of using the efficacy analysis embodied in eq 9 in the light of Murphy and Hodgson's compelling experimental evidence that surface energy participates in the chemisorption dynamics with an efficacy likely comparable to normal translational energy. Rettner and co-workers derived eigenstate-resolved dissociative sticking coefficients from associative desorption experiments using detailed balance according to eq 7 and fit the results according to the nonlinear eq 7 to extract values of $A(v, J)$, $\bar{E}_d(v, J)$, and $W(v, J; T_s)$ for each rovibrational (v, J) state. Thus, there are three nonlinear parameters extracted for each of the rovibrational states appearing in Figure 4 (19 states for H₂, 34 states for D₂). The $A(v, J)$ parameters were taken to be independent of J , and the vibrational populations of Figures 4c and 4d were used to fix the resulting $A(v)$. Consequently there are 40 and 71 semiempirically defined nonlinear parameters for H₂ and D₂, respectively, that characterize the dissociative

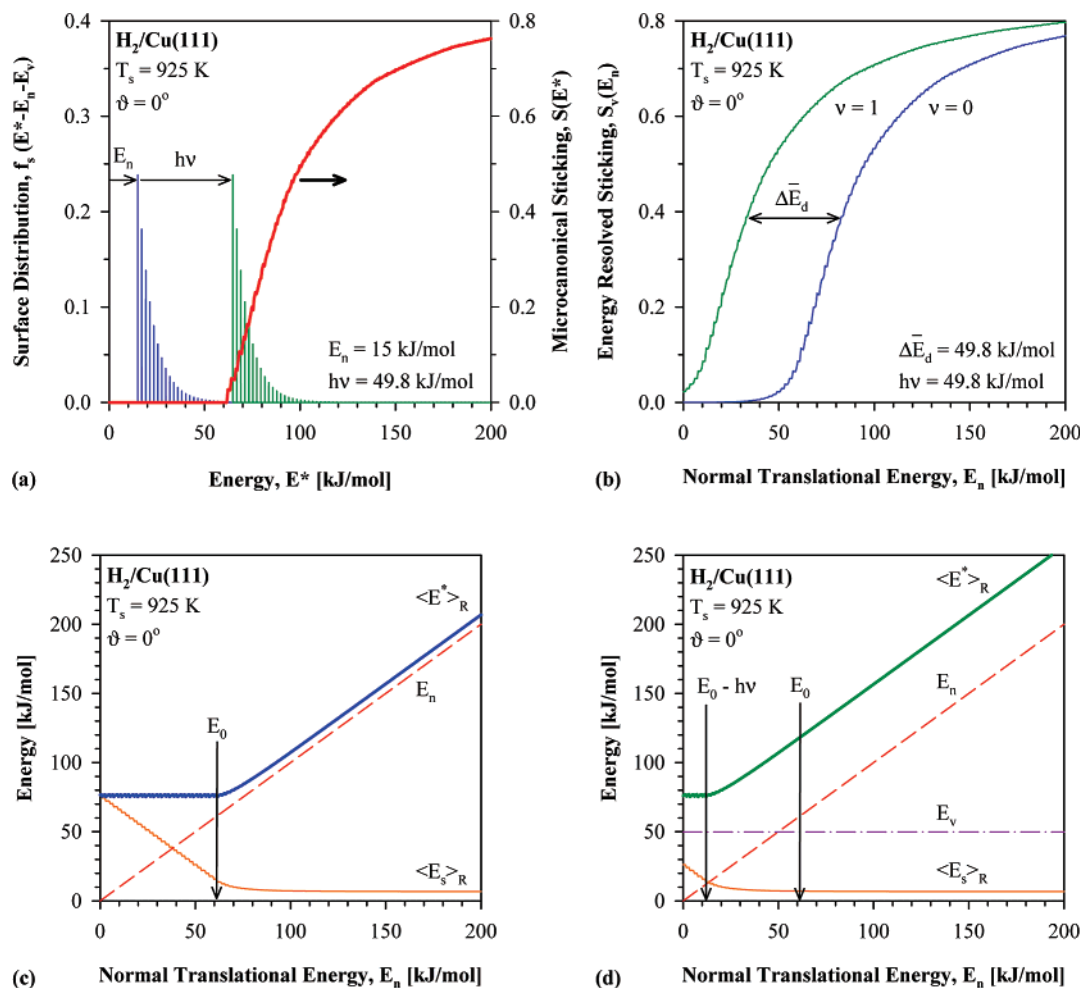


Figure 10. PC-MURT calculations of (a) the integrand components of the eigenstate-resolved sticking coefficient $S(E_i, \vartheta; E_v, E_r, T_s) = \int_{E_n + E_v}^{\infty} S(E^*) \cdot f_s(E^* - E_n - E_v) dE^*$ and (b) $S(E_i, \vartheta; E_v, E_r, T_s)$ for the ground ($E_v = 0$) and first excited ($E_v = h\nu = 49.8$ kJ/mol) vibrational states with $J = 0$ ($E_r = 0$). Mean energies derived from different degrees of freedom for the successfully reacting PCs are plotted for the relevant (c) ground and (d) vibrationally excited molecular eigenstate-resolved dissociative sticking experiments.

sticking at $T_s = 925$ K. Although these sticking parameter sets nicely reproduce the associative desorption translational energy distributions measured at $T_s = 925$ K, there is no rigorous theoretical basis (other than interpolation) by which to predict any one parameter if one knows any of the others. Murphy and Hodgson showed that at least the $W(v, J; T_s)$ parameters vary with T_s . After experimentally determining $W(v, J; T_s)$ for some values of T_s and some eigenstates, Murphy and Hodgson were unable to reproduce the Figure 3 T_s -dependent desorption angular yields and mean translation energy as a function of angle via detailed balance without positing that the effective translational energy scaling constant n was a function of E_t (requiring two additional parameters) such that $n(E_t) \approx 2$ for $E_t \geq \bar{E}_d(v, J)$ and $n(E_t)$ gradually drops to ~ 0.5 as E_t falls to zero.¹⁴ The proposed variation of the effective translational energy $E_e = E_t \cos^{n(E_t)} \vartheta$ with E_t was interpreted to mean that the PES was sufficiently corrugated parallel to the surface that parallel translational energy increasingly aids dissociation as E_t is lowered. This many-parameter erf model reproduces the D₂/Cu(111) experiments of Figure 3 about as well as the three-parameter PC-MURT model that assumes that normal energy scaling ($n = 2$) rigorously applies at all E_t . Both models slightly underpredicted the Figure 3b $\langle E_t \rangle$ values measured by Comsa and David.¹³ Given the ambiguity in the physical meaning of the “mean dynamical barrier” parameter $\bar{E}_d(v, J)$, the likely difficulty^{6,14} in accurately determining its value through fitting

dissociative sticking coefficients to the nonlinear eq 7 functional form, and the uncontrolled dynamical role of the surface in the eq 9 definition of the vibrational efficacy, it is not immediately obvious that a value of $\xi_v = 1$ will be robustly observable for systems where E_v is equally efficacious as E_e in promoting reaction. Below, we provide reassurance that, for the statistical PC-MURT, $\xi_v = 1$ should indeed be observed despite the variable dynamical role of the surface.

D.2. Sigmoid-Shaped $S(E_n, J; E_v, E_r, T_s)$. The rovibrational eigenstate-resolved dissociative sticking coefficient of eq 7 is calculated according to eqs 2–4 of the PC-MURT as

$$S(E_t, \vartheta; E_v, E_r, T_s) = \int_0^{\infty} S(E_n + E_v + E_s) f_s(E_s) dE_s \\ = \int_{E_n + E_v}^{\infty} S(E^*) f_s(E^* - E_n - E_v) dE^* \quad (10)$$

where $E_n = E_t \cos^2 \vartheta$, $E_v = E_v(v)$, $E_r = E_r(J)$, $E^* = E_n + E_v + E_s$, $S(E^*)$ is the microcanonical sticking coefficient, and $f_s(E_s)$ is the surface energy distribution for $s = 1$ surface oscillators at temperature T_s . Figure 10 illustrates how eq 10 is implemented to derive the E_t variation of $S(E_t, \vartheta = 0^\circ; E_v, E_r, T_s)$ for the H₂ rovibrational ground state ($v = 0, J = 0$) and first vibrationally ($v = 1, J = 0$) excited state and how the average energies of the successfully reacting PCs vary. Figure 10a shows that the microcanonical sticking coefficient is 0 until E^* exceeds

E_0 and its average over the surface energy distribution yields the $S(E_t, \vartheta = 0^\circ; E_v, E_t, T_s)$ sigmoid curves that depend on the value of the vibrational excitation, $E_v(\nu)$. Figure 10b shows that $S(E_t, \vartheta = 0^\circ; E_v = h\nu, E_t, T_s)$ is just $S(E_t, \vartheta = 0^\circ; E_v = 0, E_t, T_s)$ displaced backward along the E_t axis by the H_2 vibrational quantum of $h\nu = 49.8$ kJ/mol, which leads to $\xi_v = 1$. Figures 10c and 10d plot the average energy of the successfully reacting PCs, $\langle E^* \rangle_R = E_n + E_v + \langle E_s \rangle_R$, and its components for the different molecular eigenstate-resolved experiments. Figures 10c and 10d show that for $E_n + E_v < E_0$ the PCs must derive the extra energy to surmount E_0 from the surface and the average energy of the reacting PCs stays constant because of the exponential damping of the surface energy distribution. Once $E_n + E_v$ exceeds E_0 , reaction is facile, and $\langle E_s \rangle_R$ tends toward the average energy of the single surface oscillators in all of the PCs collisionally formed, $\langle E_s \rangle = k_B T_s - h\nu_s/2$, such that $\langle E^* \rangle_R \rightarrow E_n + E_v + (k_B T_s - h\nu_s/2)$. Equation 10 and Figure 10 explicitly make clear that E_n and E_v are treated symmetrically within the PC-MURT, and so their efficacies toward promoting reaction must be the same.

The eq 7 erf curve for fitting the sigmoid-shaped $S(E_t, \vartheta; \nu, J, T_s)$ has previously been loosely motivated as a semiempirical fitting form based on (i) its similarity to the transmission probability for quantum tunneling through a thin barrier in 1D⁴³ and (ii) surmounting a dynamically presented Gaussian distribution of barriers.^{50–52} Luntz explicitly shows how the second assumption can yield eq 7.⁴⁸ The PC-MURT provides a simpler TST-based derivation for why $S(E_t, \vartheta; \nu, J, T_s)$ is sigmoid-shaped and does not have an abrupt reaction threshold energy like $S(E^*)$: The eq 10 averaging of $S(E^*)$ over the surface oscillator distribution $f_s(E_s)$ is responsible. Within this over-the-barrier TST model, the sigmoid-shaped $S(E_t, \vartheta; \nu, J, T_s)$ stems from the crucial role of the surface in the dissociative chemisorption dynamics. Accordingly, Murphy and Hodgson¹⁴ found the erf $W(\nu, J; T_s)$ “width” parameter increases linearly with surface temperature, from 13.5 to 21.2 kJ/mol as T_s increased from 370 to 900 K, and is independent of J state and hydrogen isotope. Interestingly, Murphy and Hodgson¹⁴ found that fitted $\bar{E}_d(\nu = 0, J \leq 5)$ values for $H_2/Cu(111)$ were surface-temperature-independent over the range $370 \leq T_s \leq 900$ K with an average value of $\bar{E}_d(\nu = 0) = 68.5$ kJ/mol. Within the framework of the PC-MURT simulations of Figure 10b, the value of $\bar{E}_d(\nu = 0)$ will be greater than E_0 and will be dictated by the thermal averaging of $S(E^*)$ over $f_s(E_s)$ at low E_n and the similarly averaged shape and limiting value of $S(E^*)$ at high E_n .

In light of the TST derivation of the sigmoid shape of the rovibrationally resolved dissociative sticking coefficients, it is worth re-examining the likely range of applicability of the eq 7 erf function and the meaning of its parameters. According to eq 10 and Figure 10a the PC-MURT predicts that in the limit of $T_s \rightarrow 0$, $S(E_t, \vartheta; \nu, J, T_s) \rightarrow S(E^*)$ with a sudden onset as $E^* = E_n + E_v + E_s$ exceeds E_0 . Because the erf function is symmetric around $\bar{E}_d(\nu, J)$ its limiting low-temperature behavior for modeling $S(E_t, \vartheta; \nu, J, T_s)$ is markedly different than that of the PC-MURT. Although currently unavailable, eigenstate-resolved dissociative sticking experiments in the $T_s \rightarrow 0$ limit are anticipated to be difficult to fit with the eq 7 erf functional form. The PC-MURT assumes that a single reactive transition state with threshold energy E_0 at the saddlepoint along the minimum energy pathway on the PES between reactants and products can be used to define the reactive flux; there may be higher barriers on other paths but none lower than E_0 . The two eigenstate-resolved sticking experiments simulated in Figure 10b are readily interpreted within the PC-MURT framework as arising

from the need to pool sufficient exchangeable energy to exceed E_0 so that dissociative chemisorption can begin to compete against desorption as embodied by the eqs 2 and 10 average of $S(E^*)$ over the experimental flux distribution for forming PCs at energy E^* . In contrast, the “Gaussian distributions of dynamical barriers model” assumes separate barrier distributions for the $\nu = 0$ and $\nu = 1$ experiments of Figure 10b, and the connection between the barrier parameters (i.e., $\bar{E}_d(\nu, J)$ and $W(\nu, J; T_s)$) and the PES features is less clear. Thus, although the eq 9 vibrational efficacy should return a value of 1 for systems exhibiting statistical behavior, its precise meaning, other than its definition based on $\bar{E}_d(\nu, J)$ values, is not so clear for dynamical systems.

D.2. Transition State Properties. Experimental measurements of the activation energy for thermal dissociative chemisorption of H_2 on varied Cu surfaces and foils have ranged from $E_a = 36$ to 82 kJ/mol over the time frame from 1936 to 1992, as catalogued by Rettner and co-workers.⁴⁶ With some assumptions about the temperature dependence of the erf sticking parameters derived from their 925 K associative desorption experiments, Rettner and co-workers predicted the thermal activation energy for $D_2/Cu(111)$ to be 49.2 kJ/mol from 500 to 1000 K. Table 2 compares the PC-MURT thermal sticking to the experimental sticking⁴⁷ for $H_2/Cu(110)$ in the absence of modern experimental measurements for $H_2/Cu(111)$. With rotation as a spectator, the PC-MURT $E_a = 62.9$ kJ/mol ($E_0 = 62$ kJ/mol is $E_a(T = 0$ K)) is within the range reported in the past for $H_2/Cu(111)$ and is quite similar to the $E_a = 59.6$ kJ/mol experimental value measured for $H_2/Cu(110)$.

Electronic structure calculations by Hammer et al.¹⁵ of a 6D PES for $H_2/Cu(111)$ using LDA-DFT and GGA-DFT were found to display early and late barriers, respectively, for dissociative chemisorption. The LDA-DFT PES gave a reaction threshold energy that was too low, $E_0 \approx 10$ kJ/mol, whereas the GGA-DFT gave $E_0 = 48$ kJ/mol.^{20,32} One of the arguments for the physicality of the GGA-DFT PES was its late transition state, which, according to the Polanyi rules, should display increased reactivity for vibrationally excited molecules as is experimentally observed. However, only a very early barrier would display no increase in the dissociative sticking when the molecules are vibrationally excited.⁴³ The experimentally measured vibrational efficacy of $\xi_v = 0.51 \pm 0.02$ argues for an early barrier for dissociative chemisorption according to the Polanyi rules. Additional support for an early barrier stems from the experimental product state distributions for associative desorption that are similarly biased toward normal translational energy release over vibrational energy release in comparison to the statistical PC-MURT simulations. Recent GGA-DFT calculations for H_2 dissociative chemisorption on $Cu(110)$ gave $E_0 = 58$ kJ/mol¹⁹ and on Cu_m clusters⁵⁸ for $m = 4–9$ gave 36 kJ/mol $\leq E_0 \leq 142$ kJ/mol with non-monotonic variation of E_0 with m . Given the ± 20 kJ/mol likely accuracy of GGA-DFT calculations,⁸ the PC-MURT reaction threshold energy of $E_0 = 62$ kJ/mol for $H_2/Cu(111)$ is reasonable but likely should be considered an upper bound because the statistical theory does not account for the dynamically diminished vibrational efficacy. Furthermore, the eq 10 and Figure 10 analysis of $S(E_t, \vartheta; E_v, E_t, T_s)$ curves indicate that $\bar{E}_d(\nu = 0, J)$ at low J provides an upper bound for E_0 on the $H_2/Cu(111)$ PES. Experiments by Rettner et al.¹¹ yield $\bar{E}_d(\nu = 0, J = 0) = 57.1$ kJ/mol, whereas similar experiments by Murphy and Hodgson¹⁴ find negligible variation of $\bar{E}_d(\nu = 0, J)$ with J at low J and yield $\langle \bar{E}_d(\nu = 0, J \leq 5) \rangle = 68.5$ kJ/mol. The $E_0 = 62$ kJ/mol threshold energy of the PC-MURT falls just slightly below the low- J experimental average

of $\bar{E}_d(v=0, J) \approx 63$ kJ/mol, which might be considered as the experimentally based estimate of the upper bound for E_0 .

GGA-DFT calculations⁵⁹ for dissociative chemisorption of CH₄ on Ir(111) find a transition state with an Ir atom displaced 0.4 Å outward from the surface. There is a strong increase in the CH₄/Ir(111) dissociative sticking^{24,60} with increasing T_s , and it was argued⁵⁹ that increasing T_s allows more frequent access to the distorted surface geometry of the transition state that facilitates molecular dissociation. Recent 5D dynamical calculations find that the Ni(111) surface reconstructs similarly during gas–surface collisions with CH₄ and thereby lowers the barrier to dissociation.⁶¹ Figure 9 indicates that ~40% of the energy for the H₂/Cu(111) PCs to dissociate comes from the surface, and so the surface atoms preferentially involved in reaction are locally relatively hot ones that may be able to access configurations quite different than those in the static Cu(111) surface at 0 K. These observations point to the need for higher-dimensionality dynamical calculations, that explicitly include surface motion on at least a 7D PES, to make more detailed progress in understanding the H₂/Cu(111) reaction dynamics. In the meantime, the more approximate three-parameter, pseudo-7D PC-MURT model may suffice to understand and simulate many aspects of the H₂/Cu(111) dynamics, at least in a coarse-grained way.

IV. Conclusions

For a benchmark activated gas–surface reaction, a MURT local hot spot model was able to (i) provide a statistical baseline for the reactive behavior against which dynamical effects and conservation laws could be recognized, (ii) extract transition state parameters through analysis of diverse experiments, (iii) simulate the outcomes of experiments performed under non-equilibrium conditions (e.g., the $S(T_g, T_s)$ of Figure 8), and (iv) provide some insight as to how the activated reaction's energy requirements are met (e.g., f_i^* 's). We anticipate that extensions of the MURT local hot spot model to other activated condensed phase reactions will be fruitful, particularly for reactive systems with more degrees of freedom that are likely to behave more statistically.

Acknowledgment. This work was supported by the National Science Foundation (Grant No. 0415540) and by the donors of the American Chemical Society Petroleum Research Fund.

References and Notes

- Forst, W. *Unimolecular Reactions: A Concise Introduction*; Cambridge University Press: Cambridge U. K., 2003.
- Lovejoy, E. R.; Kim, S. K.; Moore, C. B. *Science* **1992**, *256*, 1541.
- Beck, R. D.; Maroni, P.; Papageorgopoulos, D. C.; Dang, T. T.; Schmid, M. P.; Rizzo, T. R. *Science* **2003**, *302*, 98.
- Smith, R. R.; Killelea, D. R.; DelSesto, D. F.; Utz, A. L. *Science* **2004**, *304*, 992.
- Liu, J. B.; Song, K. Y.; Hase, W. L.; Anderson, S. L. *J. Am. Chem. Soc.* **2004**, *126*, 8602.
- Abbott, H. L.; Bukoski, A.; Harrison, I. *J. Chem. Phys.* **2004**, *121*, 3792.
- DeWitt, K. M.; Valadez, L.; Abbott, H. L.; Kolasinski, K. W.; Harrison, I. *J. Phys. Chem. B* **2006**, *110*, 6705.
- van Santen, R. A.; Neurock, M. *Molecular Heterogeneous Catalysis: A Conceptual and Computational Approach*; Wiley-VCH: Weinheim, Germany, 2006.
- Wang, Z. S.; Darling, G. R.; Holloway, S. *Phys. Rev. Lett.* **2001**, *87*, 226102.
- Kroes, G. J.; Somers, M. F. *J. Theor. Comput. Chem.* **2005**, *4*, 493.
- Rettner, C. T.; Michelsen, H. A.; Auerbach, D. J. *J. Chem. Phys.* **1995**, *102*, 4625.
- Michelsen, H. A.; Rettner, C. T.; Auerbach, D. J.; Zare, R. N. *J. Chem. Phys.* **1993**, *98*, 8294.
- Comsa, G.; David, R. *Surf. Sci.* **1982**, *117*, 77.
- Murphy, M. J.; Hodgson, A. *J. Chem. Phys.* **1998**, *108*, 4199.
- Somers, M. F.; Kingma, S. M.; Pijper, E.; Kroes, G. J.; Lemoine, D. *Chem. Phys. Lett.* **2002**, *360*, 390.
- Perrier, A.; Bonnet, L.; Rayez, J. C. *J. Phys. Chem. A* **2006**, *110*, 1608.
- Abbott, H. L.; Harrison, I. *J. Chem. Phys.* **2006**, *125*, 024704.
- Nieto, P.; Pijper, E.; Barredo, D.; Laurent, G.; Olsen, R. A.; Baerends, E. J.; Kroes, G. J.; Farias, D. *Science* **2006**, *312*, 86.
- Salin, A. *J. Chem. Phys.* **2006**, *124*, 104704.
- Hammer, B.; Scheffler, M.; Jacobsen, K. W.; Norskov, J. K. *Phys. Rev. Lett.* **1994**, *73*, 1400.
- Kavulak, D. F.; Abbott, H. L.; Harrison, I. *J. Phys. Chem. B* **2005**, *109*, 685.
- Bukoski, A.; Blumling, D.; Harrison, I. *J. Chem. Phys.* **2003**, *118*, 843.
- Bukoski, A.; Abbott, H. L.; Harrison, I. *J. Chem. Phys.* **2005**, *123*, 094707.
- Abbott, H. L.; Harrison, I. *J. Phys. Chem. B* **2005**, *109*, 10371.
- DeWitt, K. M.; Valadez, L.; Abbott, H. L.; Kolasinski, K. W.; Harrison, I. *J. Phys. Chem. B* **2006**, *110*, 6714.
- Abbott, H. L.; Harrison, I. *J. Phys. Chem. C* **2007**, *111*, 13137.
- Wei, J. M.; Iglesia, E. *J. Catal.* **2004**, *224*, 370.
- Rauscher, H. *Surf. Sci. Rep.* **2001**, *42*, 207.
- Ukrainsev, V. A.; Harrison, I. *J. Chem. Phys.* **1994**, *101*, 1564.
- Stein, S. E.; Rabinovitch, B. S. *J. Chem. Phys.* **1973**, *58*, 2438.
- Kratzer, P.; Hammer, B.; Norskov, J. K. *Surf. Sci.* **1996**, *359*, 45.
- Sakong, S.; Gross, A. *Surf. Sci.* **2003**, *525*, 107.
- Berger, H. F.; Leisch, M.; Winkler, A.; Rendulic, K. D. *Chem. Phys. Lett.* **1990**, *175*, 425.
- van Willigen, W. *Phys. Lett. A* **1968**, *28*, 80.
- Gross, A.; Hammer, B.; Scheffler, M.; Brenig, W. *Phys. Rev. Lett.* **1994**, *73*, 3121.
- Hou, H.; Gulding, S. J.; Rettner, C. T.; Wodtke, A. M.; Auerbach, D. *J. Science* **1997**, *277*, 80.
- Gulding, S. J.; Wodtke, A. M.; Hou, H.; Rettner, C. T.; Michelsen, H. A.; Auerbach, D. *J. Chem. Phys.* **1996**, *105*, 9702.
- Dai, J. Q.; Light, J. C. *J. Chem. Phys.* **1997**, *107*, 1676.
- Dai, J. Q.; Light, J. C. *J. Chem. Phys.* **1998**, *108*, 7816.
- Gross, A.; Wilke, S.; Scheffler, M. *Phys. Rev. Lett.* **1995**, *75*, 2718.
- Polanyi, J. C.; Wong, W. H. *J. Chem. Phys.* **1969**, *51*, 1439.
- Halstead, D.; Holloway, S. *J. Chem. Phys.* **1990**, *93*, 2859.
- Darling, G. R.; Holloway, S. *Rep. Prog. Phys.* **1995**, *58*, 1595.
- Norskov, J. K.; Bligaard, T.; Logadottir, A.; Bahn, S.; Hansen, L. B.; Bollinger, M.; Bengard, H.; Hammer, B.; Sljivancanin, Z.; Mavrikakis, M.; Xu, Y.; Dahl, S.; Jacobsen, C. J. H. *J. Catal.* **2002**, *209*, 275.
- Pathria, R. K. *Statistical Mechanics*, 2nd ed.; Butterworth-Heinemann: Oxford, U. K., 1996.
- Rettner, C. T.; Michelsen, H. A.; Auerbach, D. *J. Faraday Discuss.* **1993**, *96*, 17.
- Campbell, J. M.; Domagala, M. E.; Campbell, C. T. *J. Vac. Sci. Technol., A* **1991**, *9*, 1693.
- Luntz, A. C. *J. Chem. Phys.* **2000**, *113*, 6901.
- Rettner, C. T.; Auerbach, D. J.; Michelsen, H. A. *Phys. Rev. Lett.* **1992**, *68*, 1164.
- Balooch, M.; Cardillo, M. J.; Miller, D. R.; Stickney, R. E. *Surf. Sci.* **1974**, *46*, 358.
- Rettner, C. T.; Delouise, L. A.; Auerbach, D. J. *J. Chem. Phys.* **1986**, *85*, 1131.
- Michelsen, H. A.; Auerbach, D. J. *J. Chem. Phys.* **1991**, *94*, 7502.
- Juurink, L. B. F.; McCabe, P. R.; Smith, R. R.; DiCologero, C. L.; Utz, A. L. *Phys. Rev. Lett.* **1999**, *83*, 868.
- Schmid, M. P.; Maroni, P.; Beck, R. D.; Rizzo, T. R. *J. Chem. Phys.* **2002**, *117*, 8603.
- Rettner, C. T.; Auerbach, D. J.; Michelsen, H. A. *J. Vac. Sci. Technol., A* **1992**, *10*, 2282.
- Wang, Z. S.; Darling, G. R.; Holloway, S. *J. Chem. Phys.* **2004**, *120*, 2923.
- Dohle, M.; Saalfrank, P. *Surf. Sci.* **1997**, *373*, 95.
- Guvelioglu, G. H.; Ma, P. P.; He, X. Y.; Forrey, R. C.; Cheng, H. S. *Phys. Rev. Lett.* **2005**, *94*, 026103.
- Henkelman, G.; Jonsson, H. *Phys. Rev. Lett.* **2001**, *86*, 664.
- Seets, D. C.; Reeves, C. T.; Ferguson, B. A.; Wheeler, M. C.; Mullins, C. B. *J. Chem. Phys.* **1997**, *107*, 10229.
- Nave, S.; Jackson, B. *Phys. Rev. Lett.* **2007**, *98*, 173003.